A soft-constrained Unscented Kalman Filter estimator for Li-ion cells electrochemical model

Stefano Marelli, Matteo Corno

Abstract— **Li-ion batteries require advanced Battery Management Systems (BMSs). The estimation of the cells internal quantities (residual energy, temperature, ions concentrations) is paramount for the correct and safe operation of Li-ion batteries. Accurate estimation of these quantities is however a challenging task. This work addresses the internal state estimation of a Li-ion cell applying the Unscented Kalman Filter (UKF) approach to the complete P2D model. The use of the complete P2D model allows for the estimation of the spatial distribution of Li-ions concentrations, along with the estimate of the bulk State of Charge (SoC). The paper illustrates how the UKF can address the two main issues involved in using the P2D model in estimation: weak observability and computational load. The observability issue is addressed imposing a soft mass conservation constraint in the UFK particles computation, while a parallelized implementation softens the computational burden. Extensive simulations validates the approach with currents up to 50C.**

I. Introduction

Lithium ions (Li-ion) batteries are nowadays the most widely spread technology for electric mobility and consumer electronics. They store and deliver electric energy efficiently, but because of their chemically unstable nature they need particularly advanced Battery Management Systems (BMSs) which measure, estimate, monitor and control the sate of the battery pack.

Because of inaccuracies in the estimation, the current BMS design approach is often conservative; the BMS does not exploit the full potential of the battery. The key factors in operating a Li-ion cell are essentially the need for accurate modeling, parameters identification and state estimation.

A Li-ion cell is mainly composed of a negative and positive electrode, and a separator [1]. The electrodes have a lattice structure, in which active material (i.e. lithium) is stored, and are immersed in an (usually liquid) electrolyte. The separator is an electrical insulator which allows only the Li-ions to flow through it. During discharge, lithium diffuses to the surface of active material particles of the negative electrode and it undergoes the electron-generating reaction. Then, Li-ions, dissolved in the electrolyte, cross the separator, while electrons are conducted by the solid lattice to the current collector. Finally, both Li-ions and electrons reach the positive electrode and are reabsorbed in the active material particles. This process is called *dual-intercalation* [2].

This work was supported by MIUR SIR project RBSI14STHV.

The authors are with the Department of Electronics, Information and Bioengineering, Politecnico di Milano, via G. Ponzio 34/5, 20133, Milan, Italy.

Email: {stefano.marelli,matteo.corno}@polimi.it

Li-ion cells models can be of various complexity, as shown in [3], starting from electroequivalent circuits, to advanced Computational Fluid Dynamics (CFD) models, that are extremely accurate, but at the price of high computational cost. In the aforementioned work, it was also shown how standard battery operations could be improved if limitations were applied to reactions overpotentials instead of just on terminal voltage (as done in current practice). This improvement can only be achieved if a sufficiently accurate model is selected, with insight on the electrochemical reactions taking place inside the cell. In particular, internal lithium concentration gradients represent a crucial information if one wants to effectively avoid reaching locally critical depletion levels [4]. The first-principle Pseudo 2-Dimensional (P2D) model originally formulated in [5], and later adopted in works such as [6], [7] and [2], is widely recognized as a valuable trade-off between modeling detail and computational cost. The P2D model, relying on Partial Differential Algebraic Equations (PDAEs), poses some limitation in terms of computational demands and observer formulation. The literature offers several methods to find approximated and/or reduced-order solutions [8]. For example, the Single Particle Model (SPM) [9] assumes each electrode as composed by a single spherical particle, thus neglecting the electrolyte dynamics. This model does not encompass concentrations gradients in longitudinal direction; as a consequence, it is accurate for low currents only. Another approach is to simplify the diffusion dynamics in the spherical particles radial direction. For example, [10] forces an assumption of parabolic or polynomial concentrations distribution in active material particles. Integral expressions for the response of reaction molar flux for short times and long times were, instead, introduced by [5]. Furthermore, [7] proposed a solid phase diffusion impedance model, and applied Finite Elements Method (FEM) on electrolyte phase. The present work employs a Finite Difference Method (FDM) space-discretization technique for the PDAEs as it allows for easy order rescaling and maintains the physical meaning of all the variables and parameters.

State estimation techniques reflect the complexity and accuracy of the models they employ. One of the most successful and well investigated approach employs the SPM [11]. Other works employ the P2D model by proposing different types of order reduction: [4] estimates the instantaneous available current; [12] estimates the bulk SoC using an Extended Kalman Filter (EKF) on a linearized version of the P2D model; [13] extends the estimation to the Li-ion concentrations using a Kalman Filter based on orthogonal collocation.

The nonlinear nature of the cell dynamics may be better suited for nonlinear filtering techniques: [14] investigates the use of Unscented Kalman Filter (UKF) for SoC estimation in an simple electroequivalent model, while [15] applies it to a volume-averaged electrochemical model. The previous results prove that the UKF approach [16] is an interesting tool to account for the cell nonlinear dynamics. The present work further extends the application of the UKF to the complete (i.e. not simplified) electrochemical P2D model. This not only enables the accurate estimation of bulk quantities, such as SoC, but also exploits the capability of the P2D model to estimate local concentration values in any point of the cell. The UKF approach has mainly three advantages: 1) it does not require a closed-form representation of the dynamics; this makes it very useful to avoid analytically solving the algebraic constraints, 2) it can be easily modified to account for soft-constraints that, as illustrated, improve the model observability, and 3) it is amenable to parallel implementation.

This paper is structured as follows. In Section II, the P2D model is recalled and space-discretized. In Section III, the main problems arising from applying the classical UKF to the P2D model are first introduced, then solved by implementing the concept of soft-constrained UKF; also, the results of UKF parallel implementation are shown. The new approach is fully validated in simulation in Section IV. Finally, conclusions are drawn in Section V.

II. Electrochemical model

The P2D model is widely accepted in literature [5], [7], [13]. In the P2D model, a set of PDAEs describes the dual-intercalation process. Only the diffusion dynamics that take place across the battery film thickness, indicated as *longitudinal direction x*, and the diffusion dynamics inside the spherical particles, along the *radial direction r*, are considered. Table I summarizes the conservation equations: the left column shows the original PDAEs; the right column presents the result of the proposed discretization. c_s is the concentration of lithium in solid phase; c_e is the concentration of Li-ions in electrolyte phase; i_s is the electronic current in solid phase; i_e is the ionic current in electrolyte phase; ϕ_s is the potential of solid phase; ϕ_e is the potential of electrolyte phase. D_s is the solid phase diffusion coefficient; F is the Faraday's constant; a_s is the specific interfacial area of an electrode; D_e^{eff} is the effective diffusion coefficient; t_+^0 is the transference number of Li+ (assumed as a constant); σ^{eff} is the effective conductivity; k^{eff} is the effective ionic conductivity, while k_D^{eff} is the effective diffusion conductivity. A few geometrical quantities are defined as well: A is the electrode plate area; $\delta_{n,p,s}$, are, respectively, the thickness of the negative and positive electrodes and separator; $L = \delta_n + \delta_p + \delta_s$ is the overall film thickness.

The molar flux j^{Li} at the surface of active material particles is described by the *Butler-Volmer kinetics* equation:

$$j^{Li} = a_s j_0 \left[exp\left(\frac{\alpha_a F}{RT}\eta\right) - exp\left(-\frac{\alpha_c F}{RT}\eta\right)\right] \qquad (25)$$

where $\alpha_{a,c}$ are, respectively, the anodic and cathodic transfer coefficients; R is the universal gas constant; T is the lumped cell temperature; j_0 is the exchange current density. The reaction overpotential η is defined as:

$$\eta = \phi_s - \phi_e - U(c_{se}) \qquad (26)$$

where the thermodynamic equilibrium potential U is evaluated as a nonlinear function of the surface concentration c_{se} [6]. The gradients of i_s and i_e are functions of j^{Li},

$$\frac{\partial i_s}{\partial x} = -j^{Li} \qquad \frac{\partial i_e}{\partial x} = j^{Li};$$

which satisfy the following constraints within the separator $x \in [\delta_n, \delta_n + \delta_s]$:

$$\frac{\partial i_s}{\partial x}(x) = \frac{\partial i_e}{\partial x}(x) = 0 \qquad (27)$$

$$i_s(x) = 0 \qquad (28)$$

$$i_e(x) = \frac{I}{A}. \qquad (29)$$

The terminal cell voltage is given by:

$$V = \phi_s(x = L) - \phi_s(x = 0) - \frac{R_f}{A} I \qquad (30)$$

where R_f is the film resistance of the electrode surface. In what follows, the cell parameters from [6] are considered.

The space-dicretization with FDM approach described in [12] is applied to the P2D model, as depicted in Figure 1. The negative and positive electrodes and the separator

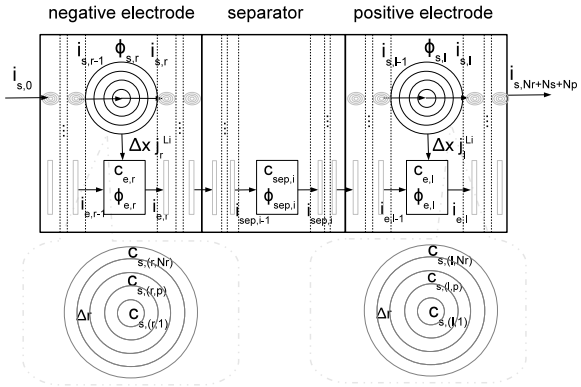

Fig. 1. Discretization of Li-ion cell along the x and r directions.

are discretized along x with, respectively, $N_{n,p,s}$ elements and spacing $\Delta x_{n,p,s}$; each spherical active material particle is further discretized along r with N_r steps spaced Δr. Thus, the electrochemical model is described by $(N_r+1)(N_n+N_p)+N_s$ Ordinary Differential Equations (ODEs), plus $5(N_n+N_p)+2N_s-3$ non-linear algebraic constraints.

Given the above model, the stoichiometry θ_s is defined as the ratio between the local value of concentration c_s and its maximum value $c_{s,max}$ [6]; and θ_{se} is the stoichiometry evaluated at an active material particle surface. SoC is defined as the average stoichiometry in negative electrode [2], normalized between two experimentally determined limits [12]:

TABLE I

ELECTROCHEMICAL MODEL: CONSERVATION EQUATIONS[1]

Species: solid phase	
$\frac{\partial c_s}{\partial t} = \frac{D_s}{r^2}\frac{\partial}{\partial r}\left(r^2\frac{\partial c_s}{\partial r}\right)$ (1)	$\dot{c}_{s,(k,p)} = \frac{D_s}{(p\Delta r)^2}\left[2p\Delta r\left(\frac{c_{s,(k,p+1)}-c_{s,(k,p)}}{\Delta r}\right) + (p\Delta r)^2\left(\frac{c_{s,(k,p-1)}-2c_{s,(k,p)}+c_{s,(k,p+1)}}{\Delta r^2}\right)\right]$ (2)
$\left.\frac{\partial c_s}{\partial r}\right\|_{r=0} = 0$ (3)	$c_{s,(k,1)} - c_{s,(k,0)} = 0$ (5)
$D_s\left.\frac{\partial c_s}{\partial r}\right\|_{r=R_s} = \frac{-j^{Li}}{a_s F}$ (4)	$D_s\left(\frac{c_{s,(k,N_r+1)}-c_{s,(k,N_r)}}{\Delta r}\right) = \frac{-j_k^{Li}}{a_s F}$ (6)
Species: electrolyte phase	
$\frac{\partial \varepsilon_e c_e}{\partial t} = \frac{\partial}{\partial x}\left(D_e^{eff}\frac{\partial c_e}{\partial x}\right) + \frac{1-t_+^0}{F}j^{Li}$ (7)	$\dot{c}_{e,k} = \frac{D_e^{eff}}{\varepsilon_e}\left(\frac{c_{e,k-1}-2c_{e,k}+c_{e,k+1}}{\Delta x^2}\right) + \frac{1-t_+^0}{F}j_k^{Li}$ (8)
$\left.\frac{\partial c_e}{\partial x}\right\|_{x=0} = 0$ (9)	
$\left.\frac{\partial c_e}{\partial x}\right\|_{x=L} = 0$ (10)	$c_{e,1} - c_{e,0} = 0$ (11)
	$c_{e,N_n+N_s+N_p+1} - c_{e,N_n+N_s+N_p} = 0$ (12)
Charge: solid phase	
$i_s = -\sigma^{eff}\frac{\partial \phi_s}{\partial x}$ (13)	$i_{s,k} = -\sigma^{eff}\left(\frac{\phi_{s,k+1}-\phi_{s,k}}{\Delta x}\right)$ (14)
$\left.\frac{\partial \phi_s}{\partial x}\right\|_{x=\delta_n} = \left.\frac{\partial \phi_s}{\partial x}\right\|_{x=\delta_n+\delta_s} = 0$ (15)	$i_{s,N_n} = i_{s,N_n+N_s} = 0$ (17)
$-\sigma^{eff}\left.\frac{\partial \phi_s}{\partial x}\right\|_{x=0} = -\sigma^{eff}\left.\frac{\partial \phi_s}{\partial x}\right\|_{x=L} = \frac{I}{A}$ (16)	$i_{s,0} = i_{s,N_n+N_s+N_p} = \frac{I}{A}$ (18)
Charge: Electrolyte Phase	
$i_e = -k^{eff}\frac{\partial \phi_e}{\partial x} - k_D^{eff}\frac{\partial}{\partial x}ln(c_e)$ (19)	$i_{e,k} = -k^{eff}\left(\frac{\phi_{e,k+1}-\phi_{e,k}}{\Delta x}\right) - k_D^{eff}\left(\frac{ln(c_{e,k+1})-ln(c_{e,k})}{\Delta x}\right)$ (20)
$\left.\frac{\partial \phi_e}{\partial x}\right\|_{x=0} = 0$ (21)	
$\left.\frac{\partial \phi_e}{\partial x}\right\|_{x=L} = 0$ (22)	$\phi_{e,1} - \phi_{e,0} = 0$ (23)
	$\phi_{e,N_n+N_s+N_p+1} - \phi_{e,N_n+N_s+N_p} = 0$ (24)

$$\mathrm{SoC} = \frac{\left(\frac{3}{\delta_n R_s^3}\int_0^{\delta_n}\int_0^{R_s} r^2\theta_s\ drdx\right) - \theta_{s,0\%}}{\theta_{s,100\%} - \theta_{s,0\%}} \tag{31}$$

where $\theta_{s,0\%}$ is the limit stoichiometry at SoC $= 0\%$, and $\theta_{s,100\%}$ is the limit stoichiometry at SoC $= 100\%$. SoC is synthetically representative for the amount of charge available inside the cell.

III. SOFT-CONSTRAINED UNSCENTED KALMAN FILTER ESTIMATOR

The UKF belongs to the family of Sigma-Point Kalman Filters (SPKFs). Details on UKF formulation and implementation, as well as considerations on theoretical aspects, can be found in [16]. To summarize, the UKF is a model-based estimator for nonlinear dynamic systems, which presents several advantages compared to other Kalman-based estimators such as EKF. In fact, it does not require any numeric/analytic computation of Jacobians, it has a computational cost similar to that of EKF, and, in turn, it is accurate to the third order of statistical moments for Gaussian systems. Additionally, its structure is inherently prone to parallel computing implementation. In the UKF algorithm, whose simplified flowchart is presented in Figure 2, a weighted set of deterministically sampled points (called *sigma-points*) is propagated by the system nonlinear state equation and used to approximate the Probability Density Function (PDF) of the state and of the output. In the case with additive process and measurement noises, these sigma-points are in the number of $2n_x + 1$,

[1]Boundary equations are marked with gray background.

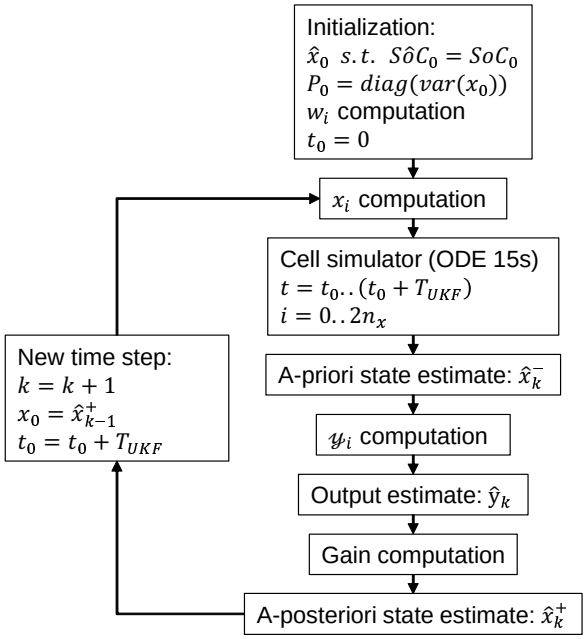

Fig. 2. UKF algorithm simplified flowchart.

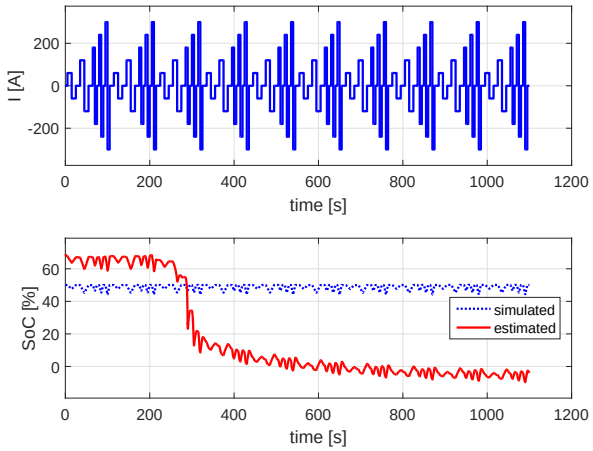

Fig. 3. Observability problem in electrochemical model: application of UKF for SoC estimation (top: input current; bottom: simulated and estimated SoC).

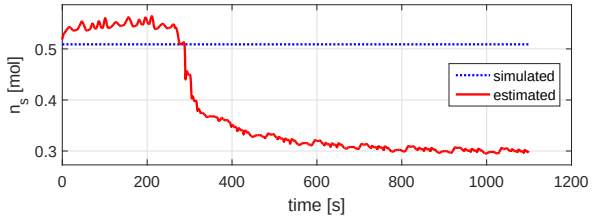

Fig. 4. Observability problem in electrochemical model: conservation of total lithium mass in solid phase, during the simulation of Figure 3.

where n_x is the dimension of the state vector; in the present work, the state vector is composed of all discretized elements of c_s and c_e, so $n_x = (N_r + 1)(N_n + N_p) + N_s$, as recalled above. The initial dispersion of these points is ruled by the covariance matrix P_0 of the initial state estimate, which is a tuning parameter. The covariance matrix Q of the process disturbance and the covariance matrix R of the measurement noise are also important tuning parameters. Minor UKF tuning parameters description can be found elsewhere [14].

A. Weak observability of P2D model

The model presented in Section II suffers from poor observability of the concentration in the core of active material particles from the output voltage, as already pointed out in [11] for SPM. The weak observability of the P2D model is confirmed by applying the classical UKF approach to the discretized P2D model with $N_r = 5$ and $N_n = N_s = N_p = 3$, using current as an input and voltage as a measured output. Figure 3 plots the estimated SoC during a current pulses cycle. In the simulation, the UKF is initialized with 20% SoC error. The figure shows that the filter does not converge. Figure 4 provides an explanation of the problem; it plots the actual and estimated number of moles of lithium available in the solid phase n_s. This is defined as the integral of c_s in the whole cell volume, i.e. both along r and along x, weighted by the solid phase volume fraction ε_s. The results proves that the sigma-point propagation mechanism does not guarantee the conservation of lithium.

To overcome the above limitation, one can modify the input-output structure of the UKF to account for the conservation of lithium. One could either follow a *hard constraint* approach, adding additional constraints in the sigma point computation that could however negatively affect the unscented distribution; or a *soft constraint* approach. The idea of the soft constraint approach is to modify the input-output structure of the model and add a *virtual* measurement, namely the total number of moles of lithium available in solid phase n_s (constant signal). In the UKF tuning, its additive measurement noise is set to have a very small variance compared to that of V. In this way, conservation of n_s is enforced as a *soft-constraint* in the estimator, and electrochemical model observability is effectively enhanced.

B. Implementation with parallel computing

The sigma-points are propagated through the nonlinear state equation independently from each other; this structure is thus amenable to parallel computing. As such, the time-update step can be optimized by distributing its computational cost on multiple cores, and the time required for this step is ultimately significantly reduced.

This advantage is quantitatively illustrated by the following computational cost analysis. Figure 5 plots the ratio between the simulation time required by the sequential and parallel implementation to run the estimator on the experiment shown in Figure 3, as a function of N_r with $N_n = N_s = N_p = 3$. Simulations were run in MathWorks MATLAB, with Parallel Computing Toolbox, on a quad-core machine (2.4GHz) with 12GB RAM and solid-state drive. From the figure, it can be concluded that the parallel implementation speeds up the estimation of a factor between 1.5 to 3 times. Note that a reduction of 4 times on a quad-core machine is not possible in practice, since the Parallel

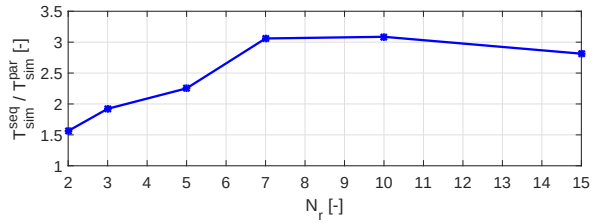

Fig. 5. Ratio between simulation time required by sequential and parallel computing implementation of UKF estimator, for different discretization levels N_r.

Computing Toolbox introduces some computing overhead to manage the information exchange among multiple solvers.

IV. Validation

This section validates the soft-constrained UKF presented in the previous sections. The filter is tested with noisy voltage measurements and the following tuning[2]:

- $N_r = 5$ and $N_n = N_s = N_p = 3$.
- The covariance matrix P_0 is a diagonal matrix, with elements on the main diagonal equal to $p_{cs} = 10^{-7}$ and $p_{ce} = 10^{-10}$;
- The covariance matrix Q is a diagonal matrix, with elements on the main diagonal equal to $q_{cs} = 10^{-11}$ and $q_{ce} = 10^{-12}$;
- The covariance matrix R is a diagonal matrix, with elements on the main diagonal equal to $r_V = 10^{-3}$ and $r_{ns} = 10^{-9}$.

Two scenarios are considered (both with voltage measurement noise):

1) a sequence of positive current pulses of 10s at 10C, starting from a fully charged cell;
2) a more dynamic test, consisting in a repeating sequence of current pulses of increasing amplitude (as high as 50C or 300A) as shown in Figure 6, starting from a fully charged cell.

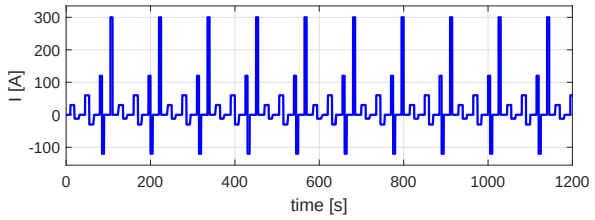

Fig. 6. Current input profile used to validate UKF: sequence of pulses at increasing amplitude (5C-10C-20C-50C in discharge).

Figure 7 and Figure 8 plot the convergence of the filter in the first test for different initial guesses of the SoC. The figure plots the bulk SoC estimate and its absolute error ε_{SoC} in percentage. The figure confirms that, even if the initialization error is very large and in the presence of a noisy voltage signal, the estimator is able to recover and finally converge to the true value of SoC. Note that, in the case with $\text{SoC}_{0,UKF} = 100\%$, ε_{SoC} keeps small for the entire duration of the test. More interestingly, Figures 9 and 10 plot the results of the estimation of lithium concentrations distributions. The former shows the convergence over different time snapshots of the estimation of surface stoichiometry for all spherical particles along x. The latter figure shows the estimate of the concentration along the radial direction. In both cases, the UKF estimate accurately describes the gradients.

[2]The tuning procedure, based on the optimization of the convergence rate and measurement noise rejection, is not described for lack of space.

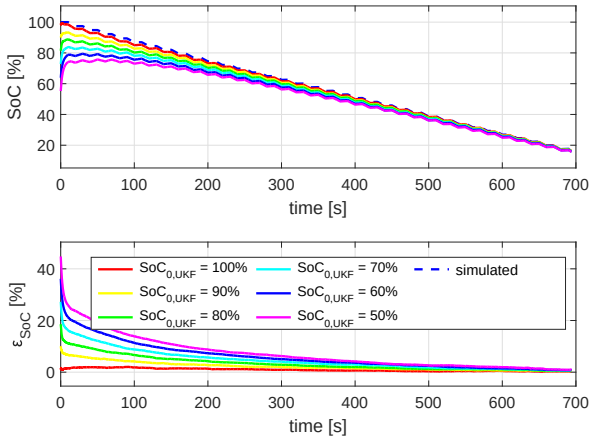

Fig. 7. Bulk SoC estimation results for the first scenario for several values of $SoC_{0,UKF}$.

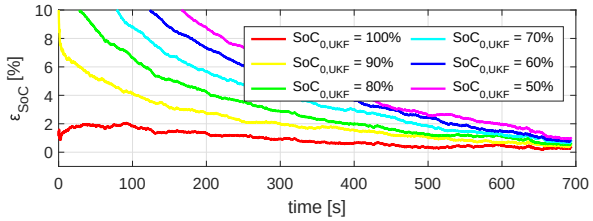

Fig. 8. Zoom on bottom sub-plot of Figure 7: for all values of $SoC_{0,UKF}$, the estimator converges on the true SoC value.

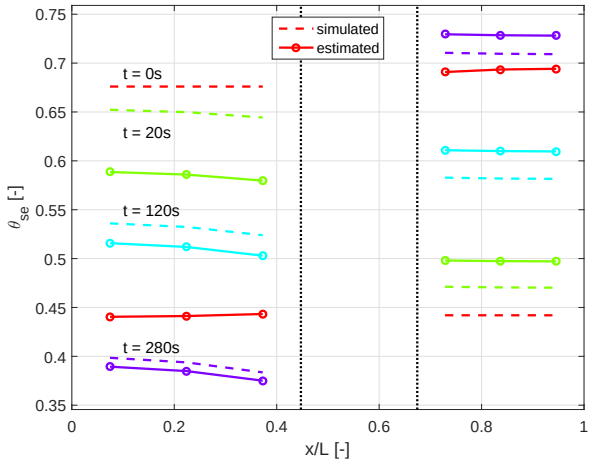

Fig. 9. Surface stoichiometry distribution along x direction, at different time instants for the first scenario. Vertical dotted lines indicate the separation among domains: negative electrode (left), separator (center) and positive electrode (right).

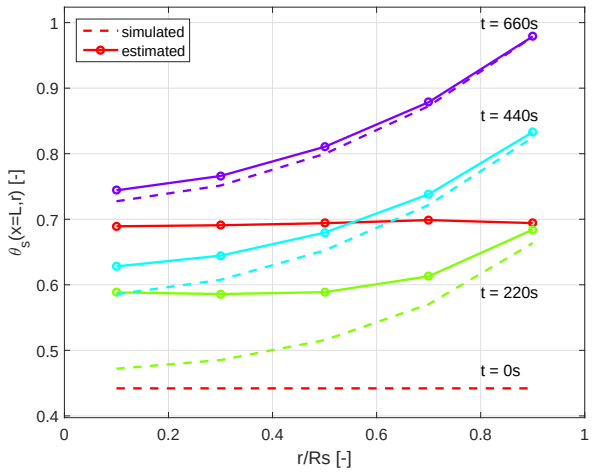

Fig. 10. Stoichiometry distribution along r direction of the spherical particle at $x = L$, at different time instants for the first scenario.

Figures 11-14 plot the results in the second scenario, following the same representation.

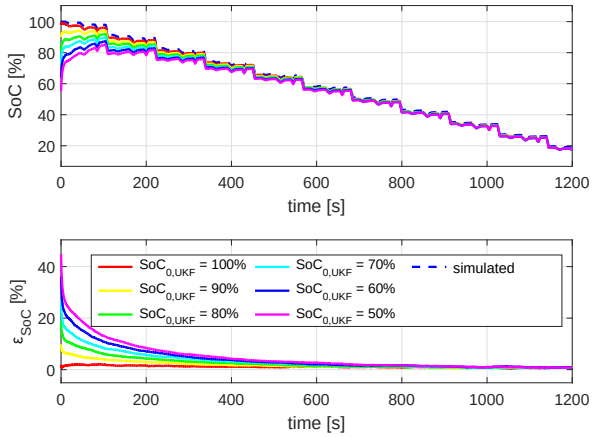

Fig. 11. Validation results for current input profile shown in Figure 6, with several values of $SoC_{0,UKF}$.

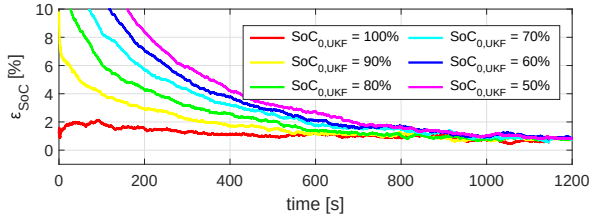

Fig. 12. Zoom on bottom sub-plot of Figure 11: for all values of $SoC_{0,UKF}$, the estimator converges on the true SoC value.

Also under this more demanding input, the estimator is able to estimate both the bulk SoC and the concentration gradients. As before, the convergence time of the bulk SoC estimation is larger when initialization error is larger, and in the case with $\mathrm{SoC}_{0,UKF} = 100\%$, ε_{SoC} keeps small for the entire duration of the test, also when very low SoC are reached. Note that in these conditions, estimating the gradients is more important as greater internal differences are triggered by the higher currents.

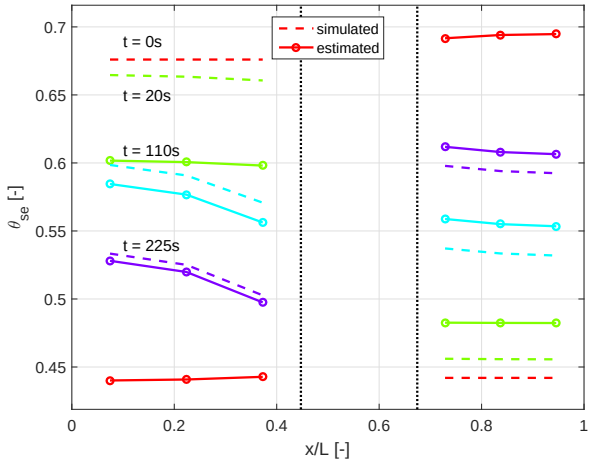

Fig. 13. Surface stoichiometry distribution along x direction, at different time instants for current input profile shown in Figure 6. Vertical dotted lines indicate the separation among domains: negative electrode (left), separator (center) and positive electrode (right).

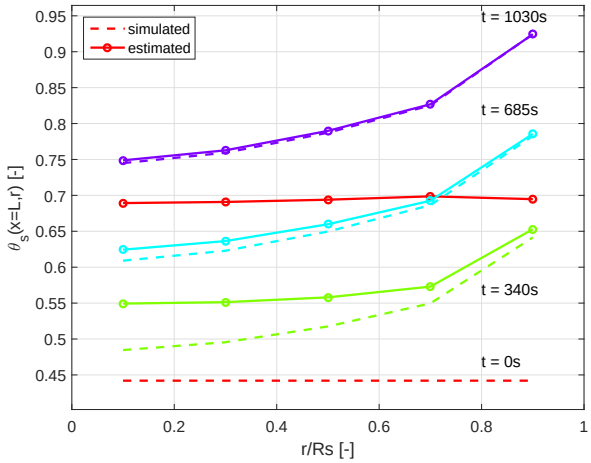

Fig. 14. Stoichiometry distribution along r direction of the spherical particle at $x = L$, at different time instants for current input profile shown in Figure 6.

V. Conclusions

The present work applies an UKF estimator to the complete electrochemical P2D model. In particular, a soft-constrained UKF allows for an accurate estimate of both bulk quantities and local gradients, overcoming the weak observability issue of the P2D model. Moreover, the estimator is implemented in a parallel computing environment, that enables to significantly reduce its computational load.

Future work includes experimental model parameters identification and validation of the proposed UKF estimator. Also, exploitation of the proposed approach in a real-world control or diagnosis application is a promising perspective.

REFERENCES

[1] Karthik Somasundaram, Erik Birgersson, and Arun Sadashiv Mujumdar. Thermal–electrochemical model for passive thermal management of a spiral-wound lithium-ion battery. *Journal of Power Sources*, 203:84–96, 2012.

[2] Nalin A Chaturvedi, Reinhardt Klein, Jake Christensen, Jasim Ahmed, and Aleksandar Kojic. Algorithms for advanced battery-management systems. *IEEE Control Systems*, 30(3):49–68, 2010.

[3] Paul WC Northrop, Bharatkumar Suthar, Venkatasailanathan Ramadesigan, Shriram Santhanagopalan, Richard D Braatz, and Venkat R Subramanian. Efficient simulation and reformulation of lithium-ion battery models for enabling electric transportation. *Journal of The Electrochemical Society*, 161(8):E3149–E3157, 2014.

[4] K. A. Smith, C. D. Rahn, and C. Y. Wang. Model-based electrochemical estimation and constraint management for pulse operation of lithium ion batteries. *IEEE Transactions on Control Systems Technology*, 18(3):654–663, May 2010.

[5] Marc Doyle, Thomas F Fuller, and John Newman. Modeling of galvanostatic charge and discharge of the lithium/polymer/insertion cell. *Journal of the Electrochemical Society*, 140(6):1526–1533, 1993.

[6] Kandler Smith and Chao-Yang Wang. Solid-state diffusion limitations on pulse operation of a lithium ion cell for hybrid electric vehicles. *Journal of Power Sources*, 161(1):628–639, 2006.

[7] Kandler A Smith, Christopher D Rahn, and Chao-Yang Wang. Control oriented 1d electrochemical model of lithium ion battery. *Energy Conversion and management*, 48(9):2565–2578, 2007.

[8] Venkatasailanathan Ramadesigan, Vijayasekaran Boovaragavan, J Carl Pirkle, and Venkat R Subramanian. Efficient reformulation of solid-phase diffusion in physics-based lithium-ion battery models. *Journal of The Electrochemical Society*, 157(7):A854–A860, 2010.

[9] Shriram Santhanagopalan, Qingzhi Guo, Premanand Ramadass, and Ralph E White. Review of models for predicting the cycling performance of lithium ion batteries. *Journal of Power Sources*, 156(2):620–628, 2006.

[10] Venkat R Subramanian, Vinten D Diwakar, and Deepak Tapriyal. Efficient macro-micro scale coupled modeling of batteries. *Journal of The Electrochemical Society*, 152(10):A2002–A2008, 2005.

[11] Scott J Moura, Nalin A Chaturvedi, and Miroslav Krstic. Pde estimation techniques for advanced battery management systems, part i: Soc estimation. In *American Control Conference (ACC), 2012*, pages 559–565. IEEE, 2012.

[12] Matteo Corno, Nimitt Bhatt, Sergio M Savaresi, and Michel Verhaegen. Electrochemical model-based state of charge estimation for li-ion cells. *IEEE Transactions on Control Systems Technology*, 23(1):117–127, 2015.

[13] Adrien M. Bizeray, Shi Zhao, Stephen Duncan, and David A. Howey. Lithium-ion battery thermal-electrochemical model-based state estimation using orthogonal collocation and a modified extended kalman filter. *CoRR*, abs/1506.08689, 2015.

[14] Gregory L Plett. Sigma-point kalman filtering for battery management systems of lipb-based hev battery packs: Part 1: Introduction and state estimation. *Journal of Power Sources*, 161(2):1356–1368, 2006.

[15] Shriram Santhanagopalan and Ralph E. White. State of charge estimation using an unscented filter for high power lithium ion cells. *International Journal of Energy Research*, 34(2):152–163, 2010.

[16] S. J. Julier, J. K. Uhlmann, and H. F. Durrant-Whyte. A new approach for filtering nonlinear systems. In *American Control Conference, Proceedings of the 1995*, volume 3, pages 1628–1632 vol.3, Jun 1995.